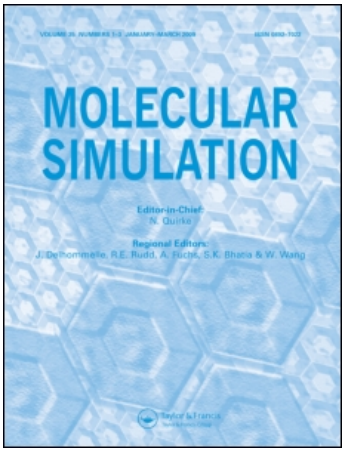

Molecular Simulation

Publication details, including instructions for authors and subscription information:
http://www.informaworld.com/smpp/title~content=t713644482

Molecular dynamics simulation of the effect of pH on the adsorption of rhodamine laser dyes on TiO_2 hydroxylated surfaces

Said Hamad[ab]; Juan Ramón Sánchez-Valencia[a]; Angel Barranco[a]; José Antonio Mejías[b]; Agustín R. González-Elipe[a]

[a] Instituto de Ciencia de Materiales de Sevilla, CSIC, Universidad de Sevilla, Seville, Spain [b] Department of Physical, Chemical and Natural Systems, University Pablo de Olavide, Seville, Spain

To cite this Article Hamad, Said , Sánchez-Valencia, Juan Ramón , Barranco, Angel , Mejías, José Antonio and González-Elipe, Agustín R.(2009) 'Molecular dynamics simulation of the effect of pH on the adsorption of rhodamine laser dyes on TiO_2 hydroxylated surfaces', Molecular Simulation, 35: 12, 1140 — 1151

To link to this Article: DOI: 10.1080/08927020903108083

URL: http://dx.doi.org/10.1080/08927020903108083

Molecular Simulation
Vol. 35, Nos. 12–13, October–November 2009, 1140–1151

Taylor & Francis
Taylor & Francis Group

Molecular dynamics simulation of the effect of pH on the adsorption of rhodamine laser dyes on TiO_2 hydroxylated surfaces

Said Hamad[ab]*, Juan Ramón Sánchez-Valencia[a], Angel Barranco[a], José Antonio Mejías[b] and Agustín R. González-Elipe[a]

[a]*Instituto de Ciencia de Materiales de Sevilla, CSIC, Universidad de Sevilla, Calle Américo Vespucio, no. 49, 41092 Seville, Spain;* [b]*Department of Physical, Chemical and Natural Systems, University Pablo de Olavide, Carretera de Utrera, km 1, Seville, Spain*

(*Received 3 February 2009; final version received 10 June 2009*)

We have carried out a study of adsorption, on the (1 0 1) surface of anatase TiO_2, of two industrially relevant rhodamine molecules [rhodamine 6G (R6G) and rhodamine 800 (R800)] employing molecular dynamics. These theoretical studies have shown that R6G must adsorb on surfaces under basic conditions. Moreover, the adsorption of this molecule shows a strong dependence upon the pH of the system, i.e. under basic conditions the adsorption energy is quite high, under neutral conditions the adsorption energy is lower and under acidic conditions an even lower adsorption energy indicates that there must be very little adsorption under such conditions. By contrast, for R800, there is little dependence of the adsorption energy upon the pH, suggesting that the amount of adsorption of these molecules is little affected by this parameter. These theoretical results are in qualitative agreement with the experimental results consisting of the incorporation of these dye molecules into porous thin films.

Keywords: rhodamine; adsorption; TiO_2; anatase; (1 0 1) surface; molecular dynamics; PZC

1. Introduction

Rhodamines are biocompatible, photostable and luminescent dye molecules, widely used for a large variety of applications including laser, probe molecule of surface states, solar cells or surface coatings [1–4]. For the majority of these uses, the dye molecule has to be incorporated into a solid, a feature that has fostered both the development of new synthesis and processing methods of the final materials and the study of their optical and fluorescent behaviours. Thus, for example, it has been shown that rhodamine-G molecules can be easily incorporated within the interlayer space of silicates and other layered materials [5–9]. The incorporation of these molecules into sol–gel silica, mesoporous TiO_2 thin films or into polymeric matrices has also been intended for the fabrication of optical components and devices [10–13].

Recently, we have shown that rhodamine 6G (R6G) and rhodamine 800 (R800) dye molecules can be incorporated within transparent and porous films of TiO_2 or Ta_2O_5, prepared by glancing angle evaporation just by immersing the films into an aqueous solution of the two dye molecules in cationic form [14]. The incorporation of the dye molecules into the film was driven by the pH of their solution and, in the case of the R6G, explained by using the classical concepts of the point of zero charge (PZC) developed in the 1960s to account for the adsorption of ions on the surface of colloidal oxides [15]. The results represent a clear evidence for the importance of the interaction of the hydroxylated porous oxide surfaces with the cationic dye molecules during absorption processes. In particular, we found that R6G only starts to be incorporated within the pores of the films when the pH of the solution was approaching or was higher than the PZC of TiO_2, i.e. around 5.5 [14,15]. The simplicity of the experimental method used for the preparation of these composite thin films has motivated the present theoretical work, where we account for the different effect of the pH and on the adsorption of R6G and R800 on the surface of TiO_2. For this purpose, we present here a theoretical study by using molecular dynamics (MD) techniques to obtain information about the adsorption of these two dye molecules. The results obtained can be of relevance for the study of other types of composite materials consisting of dye molecules adsorbed on the surface of TiO_2. A classical example in this respect is that of the Grätzel solar cells [16,17]. In this context, previous theoretical studies in the literature have dealt with the adsorption of Ru(II)-polypyridyl dyes on the surface of an ideal TiO_2 surface [18]. However, to our knowledge, no theoretical studies have been carried out to investigate the interaction of these or similar dye molecules with a hydroxylated surface of this oxide, taking into account the effect of pH on their adsorption. For the present study, we have used four different types of surfaces, on which to model the adsorption of the rhodamine molecules. The chosen models of surfaces provide a description of the adsorption

*Corresponding author. Email: said.hamad@icmse.csic.es

ISSN 0892-7022 print/ISSN 1029-0435 online

DOI: 10.1080/08927020903108083
http://www.informaworld.com

on non-hydroxylated surfaces, as well as on surfaces under basic, neutral and acidic conditions.

2. Computational details

The first step in any MD simulation is the compilation of an adequate set of interatomic potentials to model the system. Our experimental observations require the use of computational features, which are somehow more complicated than those of usual MD simulations, since we need to model the influence of hydroxylation and pH. TiO_2 surfaces are usually modelled as clean, non-hydrated and non-hydroxylated surfaces, although there are some exceptions in the literature [23–27]. The initial set of parameters used to model the TiO_2 (1 0 1) anatase surface was taken from the modification that Predota et al. [23,28] made of the Matsui and Akaogi [29] potentials to study (1 1 0) rutile hydroxylated surfaces. The parameters presented by Predota et al. [23,28] were not optimised to model the hydroxylated (1 0 1) anatase surface, and when they were used to minimise the surface, we observed the rupture of O—H bonds upon minimisation. Therefore, some changes were introduced into the interatomic potentials to allow us to study the hydroxylated (1 0 1) anatase surface. In order to have a reference to test the results of the changes of the interatomic potentials parameters, we carried out the optimisation of a hydroxylated (1 0 1) anatase surface with the density functional theory (DFT), using the plane-wave pseudo-potential approach within the projector augmented wave method [30], together with the generalised gradient approximation exchange correlation functional proposed by Perdew et al. [31], as implemented in the Vienna *ab initio* simulation package (VASP) 4.6 code [32–34]. A plane-wave cut-off energy of 400 eV was used. The Ti (3s, 3p, 3d, 4s), O (2s, 2p) and H (1s) electrons were treated as valence states, while the remaining electrons were kept frozen as core states. The Brillouin-zone integrations were performed using Monkhorst–Pack grids [35]. The slab approximation was used to model the surface with a TiO_2 slab thickness of 20 Å and a vacuum slab of 10 Å. The cell dimensions are 5.44 Å × 3.78 Å × 30.0 Å. The calculations were carried out by using a (7 × 7 × 1) mesh, with which convergence in energy was achieved.

In order to get a good agreement with the geometries obtained with the DFT calculations, we made some modifications in the interatomic potentials. Since one of the requirements was the modelling of the O—H bonds at the surface (such as bonds 2–3 and 4–5 in Figure 1), we introduced a harmonic force between the O and H atoms of the surface hydroxyl groups of the form $E = 1/2k_1(r - r_o)^2$. The values of the parameters were $k_1 = 500.4\,\text{kcal mol}^{-1}\,\text{Å}^{-2}$ and $r_o = 0.95$ Å. Another important parameter in the description of the surface

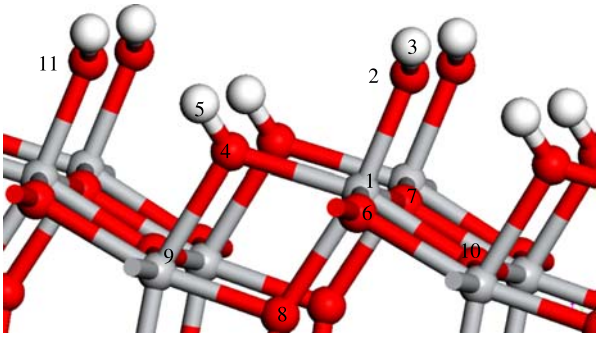

Figure 1. A close view of the hydroxylated (1 0 1) anatase surface. Red balls represent O atoms, grey balls represent Ti atoms and white balls represent H atoms.

is the harmonic force that predicts a correct value of the Ti—O—H angles (such as the angles 1–2–3 and 1–4–5 in Figure 1). This force is of the form $E = 1/2k_2(\theta - \theta_o)^2$, where θ is the angle between the three atoms, θ_o is the equilibrium value of this angle around which θ oscillates and k_2 is the constant of the harmonic force that induces these oscillations. For O—H groups connected to terminal Ti atoms, we did not change the parameters, but for O—H groups where the O involved is a bridging O (such as atom 4 in Figure 1), the new parameters are $k_2 = 14.136\,\text{kcal mol}^{-1}\,\text{rad}^{-2}$ and $\theta_o = 120°$. The geometry of the hydroxylated (1 0 1) anatase surface obtained with this new set of interatomic potentials is in reasonable good agreement with that obtained with DFT calculations, as shown in Table 1. The larger disagreement, as expected, is found for the distance between atoms 5 and 11, since they interact by a weak hydrogen bond, a situation which is difficult to model accurately using interatomic potentials.

To model the rhodamine molecules, we have employed the DREIDING force field [36], which was developed to predict structures and dynamics of organic, biological and main group inorganic molecules. The van der Waals parameters of the DREIDING force field are taken from the Williams potentials [37,38], including some modifications. The electrostatic charges were calculated with *ab initio* calculations by fitting the electrostatic potential at points selected according to the Merz–Singh–Kollman scheme [39,40], as implemented in the program Gaussian 03 [41]. The Becke three-parameter hybrid functional [42] (B3LYP) was used to fit the atomic charges together with a 6-31+G* basis set. Tables S1 and S2 show the atomic charges as well as the force type assignments. This level of theory has been previously used to study other dyes [43]. The DREIDING force field predicts an equilibrium angle of ~40° between the xanthene and phenyl moieties that form the R6G molecule, whereas *ab initio* calculations predict that the planes of the two moieties lie perpendicular to each other. In order to predict correctly this angle of 90°, we included

Table 1. Values of some of the important geometrical features of the (1 0 1) hydroxylated anatase surface, obtained with DFT and with the interatomic potentials developed by Predota et al. [23,28], including the new terms that improve the description of the O—H bonds for this particular surface.

	Torsional angle 10–1–4–5 (°)	Distance 1–2 (Å)	Distance 2–3 (Å)	Distance 4–5 (Å)	Distance 5–11 (Å)	Angle 1–4–5 (°)	Angle 1–2–3 (°)
Predota et al. [23,28] plus added terms	126.2	1.93	1.01	0.97	2.73	127.8	119.8
DFT	122.3	1.87	0.98	0.98	2.49	126.2	118.3

an additional torsional term in the force field. In DREIDING, the torsion interaction for two bonds (those between atoms IJ and KL) connected via a common bond JK takes the form

$$E_{\mathrm{IJKL}} = \frac{1}{2} V_{\mathrm{JK}} \left\{ 1 - \cos\left[n_{\mathrm{JK}} (\varphi - \varphi^0_{\mathrm{JK}}) \right] \right\},$$

where φ is the dihedral angle (angle between the IJK and JKL planes), n_{JK} is the periodicity (an integer), V_{JK} is the barrier for rotation (always positive) and φ^0_{JK} is the equilibrium angle. We did not carry out a parameter fitting in order to obtain the value of the parameters needed to model correctly the angle between the two moieties. Instead, we introduced an additional term, taking the same parameters that describe the torsion of a dihedral resonance bond (bond order = 1.5) involving two resonant atoms, namely $V_{\mathrm{JK}} = 25\,\mathrm{kcal\,mol^{-1}}$, $n_{\mathrm{JK}} = 2$, and changing the equilibrium angle from $\varphi^0_{\mathrm{JK}} = 180°$ to $\varphi^0_{\mathrm{JK}} = 90°$. This torsional force is only included to model the interaction between atoms C9 and C14 in Figure 2(a). We checked the validity of this term by comparing the variation of the energy with respect to the rotation angle, the latter obtained with the interatomic potentials discussed and two *ab initio* methods: B3LYP/6-31+G* and MP2/6-31++G**. The results are shown in Figure 3. In the most critical region, between 90° and 110°, the three methods predict essentially the same dependency with respect to the rotation. For angles higher than 110°, the less accurate methods (interatomic potentials and B3LYP/6-31+G*) predict a different change in energy than MP2/6-31++G**, although at 120° the energy difference is still $< 3\,\mathrm{kcal\,mol^{-1}}$. We can therefore consider that the DREIDING force field, with this additional term, predicts correctly the behaviour of R6G. In the case of R800, there is no need to include any additional terms, since the DREIDING force field describes it correctly. The van der Waals interactions between the rhodamine molecules and the surface are taken from the DREIDING force field. The existence of parameters to describe the interaction between the molecules and the TiO_2 surface (which is not the case for other force fields such as AMBER or CHARMM) is the main reason why the DREIDING force field is used.

All interatomic potentials-based energy minimisations and MD simulations have been performed with the GULP code [44], at the high-performance computing facilities of CSIC in Madrid. The time step for the integration of the equations of motion is 1 fs. The systems are modelled in the canonical (NVT) ensemble, employing the Hoover thermostat, with a friction constant for the temperature bath of 0.1, to maintain the temperature around 298°C. The systems are equilibrated for 50 ps, followed by 100 ps of production. Since the number of degrees of freedom associated with the motion of the rhodamine molecules is relatively small, there is no need to perform very long simulations to sample the most relevant region of the phase space.

The *ab initio* calculations (using Gaussian 03 and VASP) have been carried out in the Finis Terrae supercomputer in Santiago de Compostela, Spain.

3. Materials, theoretical results and discussion

3.1 Experimental details and materials

Composite R6G/TiO_2 and R800/TiO_2 thin films were prepared by using porous TiO_2 thin films as host materials. For this purpose, transparent and amorphous TiO_2 were prepared by glancing angle physical vapour deposition at room temperature on quartz and silicon substrates. Evaporation was carried out in an electron bombardment evaporator using TiO_2 pellets as target material. Stoichiometric thin films of TiO_2 were obtained by performing the evaporation in 10^{-4} torrs of O_2. The evaporation was carried out by placing the substrates at a glancing angle of 70° with respect to the evaporator source. This geometry produces films with a tilted-columnar microstructure and a high porosity [19–21]. Thin films with a thickness around 400 nm were prepared following this method. In the present case, the porosity of the films was estimated to be 35% of the total volume of the films with 70% of pores consisting of mesopores. A full account of the characteristics of these films can be found in a previous publication [14].

The microstructure of the TiO_2 thin films deposited on a silicon wafer was examined by field emission scanning electron microscopy in a Hitachi S5200 microscope.

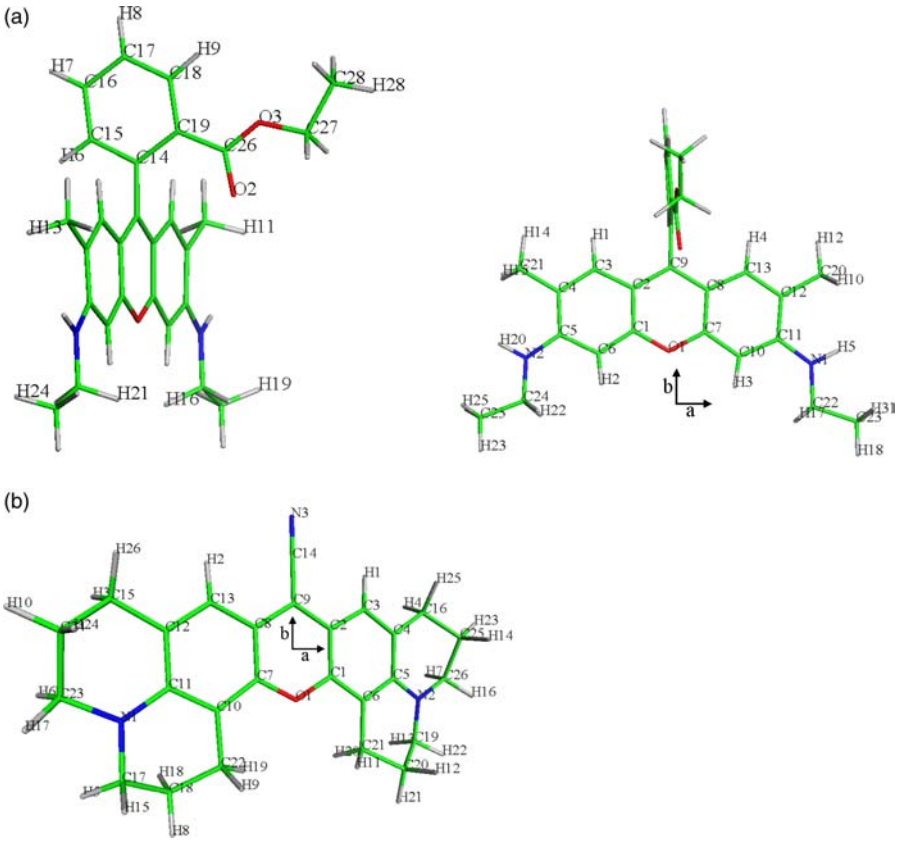

Figure 2. (a) Two views of a R6G molecule. (b) A view of a R800 molecule. The figures show the numbering assigned to each atom, which are used to assign the force field atom types and charges in Tables S1 and S2. The molecular axes *a* and *b* are also shown. In both figures green, blue, red and white sticks represent C, N, O and H atoms, respectively.

Cross-sectional views were obtained by cleaving the silicon substrates.

UV–vis absorption spectra in transmission mode were recorded with a Perkin-Elmer Lambda 12 spectrometer for the thin films deposited on quartz plates. Although the absorbance is the typical magnitude used for presenting UV–vis absorption spectra of dyes in liquid solutions, we present here some spectra as the percentage of transmitted light. We have made this choice because this is the usual way of presenting these data when using optical thin films [22].

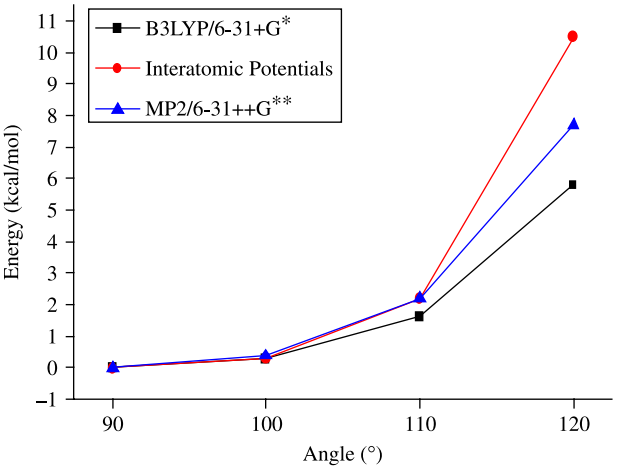

Figure 3. Change in energy as the angle between the xanthene and phenyl moieties is changed, calculated with two *ab initio* methods (B3LYP/6-31+G* and MP2/6-31++G**) and with the classical interatomic potentials used in this study.

A chloride salt of R6G and R800 dye molecules was used for the experiments. The salts were supplied by ALDRICH and used without further purification. In solution, the cationic R6G or R800 bears a positive charge, a feature that is essential for the incorporation of the dye into the TiO_2 thin films.

Solutions of 10^{-4} M of the dyes in water at controlled values of pH were used for the infiltration experiments. The pH of the solution was maintained between 1.9 and 6.6 by adding given amounts of HCl or NaOH. The TiO_2 films were immersed in one of these solutions and maintained there for 10 min. The samples were then removed from the solution and washed with water at the same pH than that of the dye solutions. In general, the intensity of the colour of the films changed with the pH of the solution, a feature that suggests the dependence between this parameter and the ability to incorporate the dye molecules into the films.

Figure 4 shows a series of UV–vis transmission spectra recorded for TiO_2 thin films containing different concentrations of R6G and R800, as indicated in Table 2. The spectra are characterised by the presence of a series of bands typical of the R6G dye molecules (i.e. bands centred at ~520 nm) and R800 (i.e. bands centred at ~650 nm) [14] superimposed on the typical oscillations due to interference phenomena between a substrate and a transparent layer of different refraction index [14]. For the purposes of the present work, the most important result is the dependence of the intensity of the features attributed to the two dye molecules and the pH of the solution used for the preparation of the films. Thus, it is observed that the intensity of the R6G features is strongly dependent on the pH, increasing with this parameter. By contrast, R800 is almost insensitive to this parameter and the intensity of its spectral features remains almost invariable for all the pHs. This different behaviour suggests that these two molecular cations interact differently with the surface of TiO_2 and that, particularly for the R800, the state of charge on the TiO_2 does not significantly affect the adsorption of this molecule.

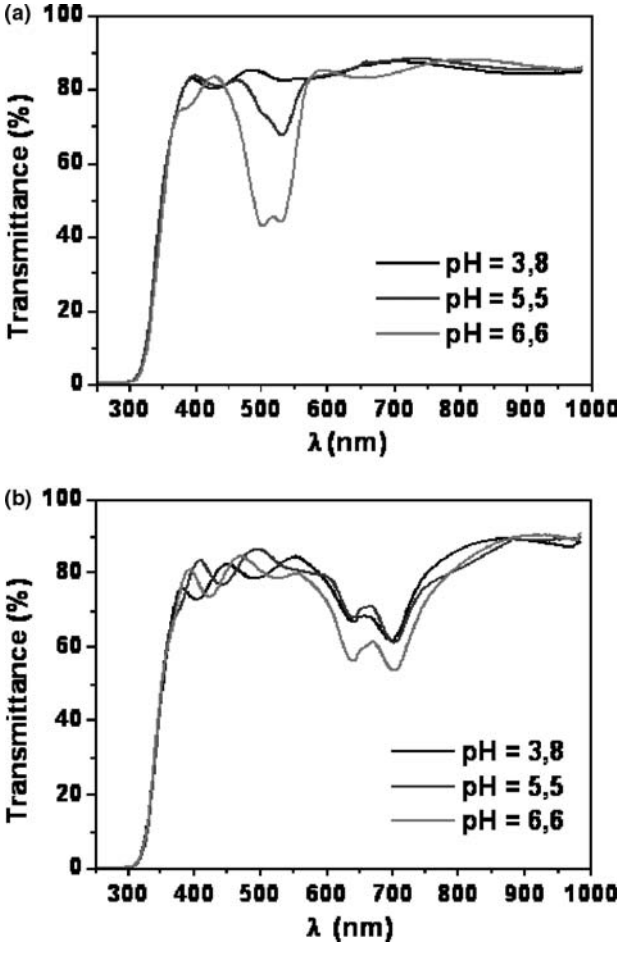

Figure 4. UV–vis transmission spectra of TiO_2 thin films with (a) R6G and (b) R800 molecules adsorbed at three different pH values.

Table 2. Concentration of the adsorbed dyes in the porous TiO_2 thin films as a function of the pH.

	Dye concentration (mol cm^{-2} nm^{-1} 10^{-12})		
pH	3.8	5.5	6.6
TiO_2–Rh6G	0	2.87	13.07
TiO_2–Rh800	5.82	4.12	7.85

3.2 *Theoretical results and discussion*

Once a suitable set of interatomic potentials is obtained, we created the unit cells that model the systems of interest. The simplest cell to study the adsorption of rhodamines is a bare surface formed by a slab of TiO_2 in vacuum. We generated a 17 Å slab exposing the (1 0 1) surface of anatase TiO_2 with a $(6a_x \times 8a_y)$ periodic replication of the experimental elementary cell of dimensions $a_x = 5.44$ Å and $a_y = 3.776$ Å. The experimental elementary cell contains 10 Ti atoms and 20 O atoms, giving a total of 480 Ti atoms and 960 O atoms in our simulation unit cell. The dimensions of the unit cell are 32.66 Å × 30.2 Å × 50 Å and the angle between a_x and a_y is 110.30°. There is a vacuum gap of 33 Å between the slabs. The charges on the Ti and O atoms are $2.196e$ and $-1.098e$, respectively. Since we are interested in studying the effect of pH on the adsorption energy (E_{ad}) of rhodamines, we also generated three unit cells to model different values of pH: (1) hydroxylated surface under neutral conditions; (2) hydroxylated surface under acidic conditions and (3) hydroxylated surface under basic conditions. Surface 1 is created by adding an H atom to each bridging O atom and a hydroxyl to each Ti atom, as shown in Figure 1. The charge of the O atoms in the hydroxyl groups is $-0.848e$ and the charge of the H atoms is $0.424e$. To model surface 2, we take into account that at low pHs there will be a large number of H atoms available to interact with the surface. The following or a similar process will happen readily:

$$\text{Surf-TiOH} + \text{H}^+ \rightarrow \text{Surf-Ti}^+ + \text{H}_2\text{O}, \qquad (1)$$

i.e. a proton from the acidic solution will interact with a hydroxyl group at the surface and form a water molecule, which will then move into the solution. Once the surface is dried, this water molecule is removed from the surface and our model of a TiO_2 surface in acidic conditions will have a positive charge of $+1e$ left in the surface. Since the charge of the hydroxyl group removed from the surface is only $-0.424e$, there will be an additional $+0.576e$ to be distributed among the atoms of the surface. This charge was distributed among the surface atoms as shown in Table 3. Surface 3 is created taking into account a different process occurring in the basic solution. Since, under these conditions, there is a large amount of OH^- groups, the

Table 3. Charges of all the atoms involved in the defects appearing at high and low pH, as well as the charges of the atoms of the hydroxylated surface under neutral conditions.

Atom	Charge in basic conditions	Charge in neutral conditions	Charge in acidic conditions
1-Ti	2.124	2.196	2.268
2-O	−0.920	−0.848	No atom
3-H	0.352	0.424	No atom
4-O	−1.170	−1.098	−1.026
5-H	No atom	0.424	0.496
6-O	−1.170	−1.098	−1.026
7-O	−1.170	−1.098	−1.026
8-O	−1.170	−1.098	−1.026
9-Ti	2.124	2.196	2.268
10-O	−1.098	−1.098	−1.026

following process will take place:

$$\text{Surf-Ti—OH} + \text{OH}^- \rightarrow \text{Surf-O}^- + \text{H}_2\text{O}. \qquad (2)$$

Thus, the result of the interaction between the hydroxylated surface and the OH^- species from the solution is the removal of one proton from the surface to form a water molecule. This water molecule will be removed into the basic solution, leaving a bridging O at the surface and a charge of $-1e$, distributed among the atoms as shown in Table 3. Processes (1) and (2) are similar to the common mechanisms considered within the PZC theory of oxides [15].

3.2.1 *Adsorption of R6G*

The UV–vis spectra shown in Figure 4(a) suggest that the maximum adsorption of R6G molecules will occur under basic conditions. This experimental behaviour is not unexpected, since these dye molecules are positively charged, and there will be an electrostatic attraction between this charge and the negative charge present on the surface due to the basic solution. As the pH decreases, the amount of negative charges on the surface decreases and therefore the adsorption decreases. When the pH is below the PZC, the surface is positively charged, a situation that must produce an electrostatic repulsion between the positive charge of the rhodamine molecule and the positive charges on the surface induced by the proton adsorbed from the acidic solutions. This general trend is also observed in the simulations. Figure 5 shows a snapshot of the simulation of the adsorption of R6G on a fully hydroxylated surface, modelling the surface for neutral conditions. As shown in Table 4 (where the values of the energies of adsorption of the two rhodamine molecules on the four types of surfaces are shown), under basic conditions, the adsorption energy of R6G is $-46.5\,\text{kcal mol}^{-1}$. Under neutral conditions, E_{ad} decreases to $-28.6\,\text{kcal mol}^{-1}$ and under acidic conditions it decreases further to $-7.1\,\text{kcal mol}^{-1}$. The latter value is negative, suggesting that there might be some adsorption of R6G under acidic conditions, in disagreement with what is experimentally observed. This apparent contradiction might be due to the simplicity of the model. E_{ad} is calculated as the difference in energy between two states. One state consists of two systems, the isolated TiO_2 surface and the isolated rhodamine molecule. The other state consists of the rhodamine molecule adsorbed onto the surface. A more accurate value of E_{ad} would be obtained if the interaction of the rhodamine molecule with water molecules would have been taken into account accurately. The interaction of rhodamine–water would cause a decrease in the adsorption energies of the two rhodamine

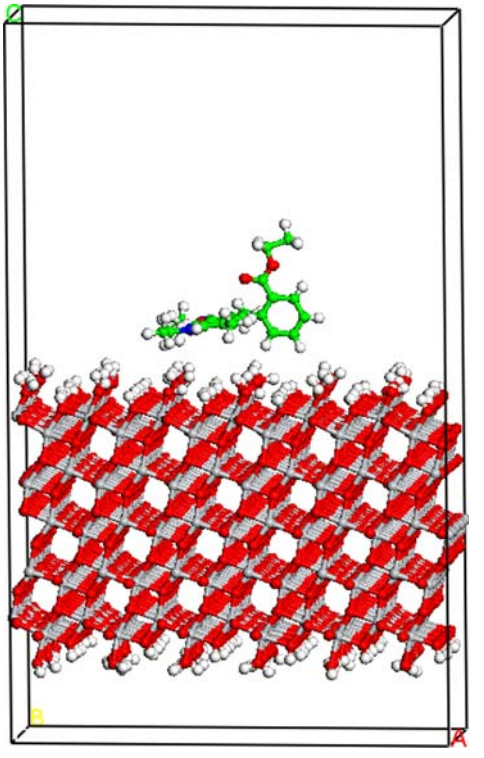

Figure 5. Ball and stick view of the simulation cell used to study the adsorption of R6G in a fully hydroxylated surface, under neutral pH conditions. Green, blue, red, white and grey ball atoms represent C, N, O, H and Ti atoms, respectively.

Table 4. Energies of adsorption, E_{ad}, of the two rhodamine molecules studied on the (1 0 1) surface of anatase.

	Acidic	Neutral	Basic	Non-hydroxylated
R6G	−7.1	−28.6	−46.5	−51.0
R800	−29.4	−33.2	−51.6	−56.7

Note: All energies are in kcal mol^{-1}.

molecules under all pH conditions. For this reason, this initial study only provides qualitative information about the general trends of adsorption energy, predicting relative energetic differences, not the actual absolute values of adsorption energy.

The dynamics of the R6G molecule adsorbed onto the different surfaces shows significant variations.

In Figure 6, the values of the (x,y) coordinates of some relevant atoms of the molecule are plotted. The shape of the cell (from a top view) is also shown. In Figure 6(a), we can see the (x,y) values of the atom H7 of the R6G when adsorbed on the bare, non-hydroxylated surface. The adsorption energy, in that case −51.0 kcal mol^{-1}, is higher than that of the other three cases in which the surface is hydroxylated. But there are no experimental results to be compared with these data, since bare TiO_2 surfaces are quickly hydrated and hydroxylated. The set of points are scattered over a wide range of values, indicating that the attraction between the molecule and the surface is evenly distributed over the surface, i.e. it is very easy for the molecule to hop around the surface. Under basic conditions, we observe the opposite effect: there is a strong attraction towards the negatively charged surface defect, a feature which creates a preference for the molecule to stay around it. In Figure 6(b), we see the (x,y) values of the atoms O1 and H7, as well as the position of the O atom that has lost its H due to the basic solution. The positions of the O1 and H7 atoms are localised in small areas, indicating that the molecule does not diffuse easily once it is absorbed. Under neutral conditions [Figure 6(c)], the mobility of the molecule is higher, and E_{ad} is lower, −28.6 kcal mol^{-1}, a result that agrees with the experimental observations. Under acidic conditions, the mobility is still higher, as suggested by the scattered set of points corresponding to the movement of the H7 atom [Figure 6(d)]. The molecule moves around the Ti atom, which has lost its hydroxyl group, and is part of the positively charged defect. During the simulation, the phenyl moiety of the R6G molecule is often inserted within the region previously occupied by the hydroxyl group. E_{ad} is now −7.1 kcal mol^{-1}, a value which is much smaller than in the case of adsorption under neutral conditions. The most relevant geometric parameters that describe the adsorption of the R6G molecules are the angles α and β. α is defined as the angle between the axis a of the molecules (which is shown in Figure 2) and the z axis of the unit cell. Analogously, β is the angle between the molecular axis b and the z axis. A value of 90° in both angles would correspond to an adsorption geometry in which the molecule lies parallel to the surface. The convention we have used to calculate the angles means that an angle lower than 90° implies that the corresponding molecular axis (a or b) points upwards, and vice versa. Figure 7 shows the values of the angles α and β during the simulations, for the two rhodamine molecules at the four conditions of pH studied.

The average values for the whole simulations are shown in Figure 8. For R6G, the average value of the angle α is very close to 90° in all cases. The larger deviation is found for the adsorption under basic conditions. The value of 88° obtained suggests an adsorption almost parallel to the surface. The angle β is more affected by the presence of the phenyl group, which has the effect of decreasing the adsorption angle of the molecule. As a result, the average value of the angle β ranges from 80.7°, in the case of non-hydroxylated surface, to 84.0° for the adsorption under acidic conditions. This higher angle for acidic conditions is due to the mentioned ability of the molecule to introduce the phenyl moiety within the region previously occupied by the removed hydroxyl group, a feature which permits a more parallel adsorption. This is also the reason why the average distance from the centre of mass of the R6G molecule to the H atoms of the surface is shorter in acidic than in neutral and basic conditions, although the presence of the phenyl moiety causes all these average distances to be higher than in the case of the adsorption of R800 (Figure 9)

3.2.2 *Adsorption of R800*

The experimental observations suggest that the adsorption of R800 is less affected than the R6G by changes in the pH of the surface, although the maximum adsorption also takes place under basic conditions and the minimum under acidic conditions. The values of the energies of adsorption calculated from the simulations for basic, neutral and acidic conditions are −51.6, −33.2 and −29.4 kcal mol^{-1}, respectively. The difference between the energies for neutral and acidic conditions is just 3.8 kcal mol^{-1}, almost five times smaller than the difference between the values for neutral and basic conditions, which is 18.4 kcal mol^{-1}. This effect is in agreement with the observation that a low pH only produces a small decrease in the intensity of the UV–vis adsorption bands [see Figure 4(b)]. The simulations provide some hints to understand the reasons for this behaviour. As it happens for R6G, under basic conditions, E_{ad} is higher because the negative charge of the surface site defect modelling the basic conditions attracts the positive charge of the molecule. The N atom of the nitrile group of the rhodamine R800 molecule [N3 in Figure 2(b)] has a negative charge of −0.417e. Therefore, the negatively charged site

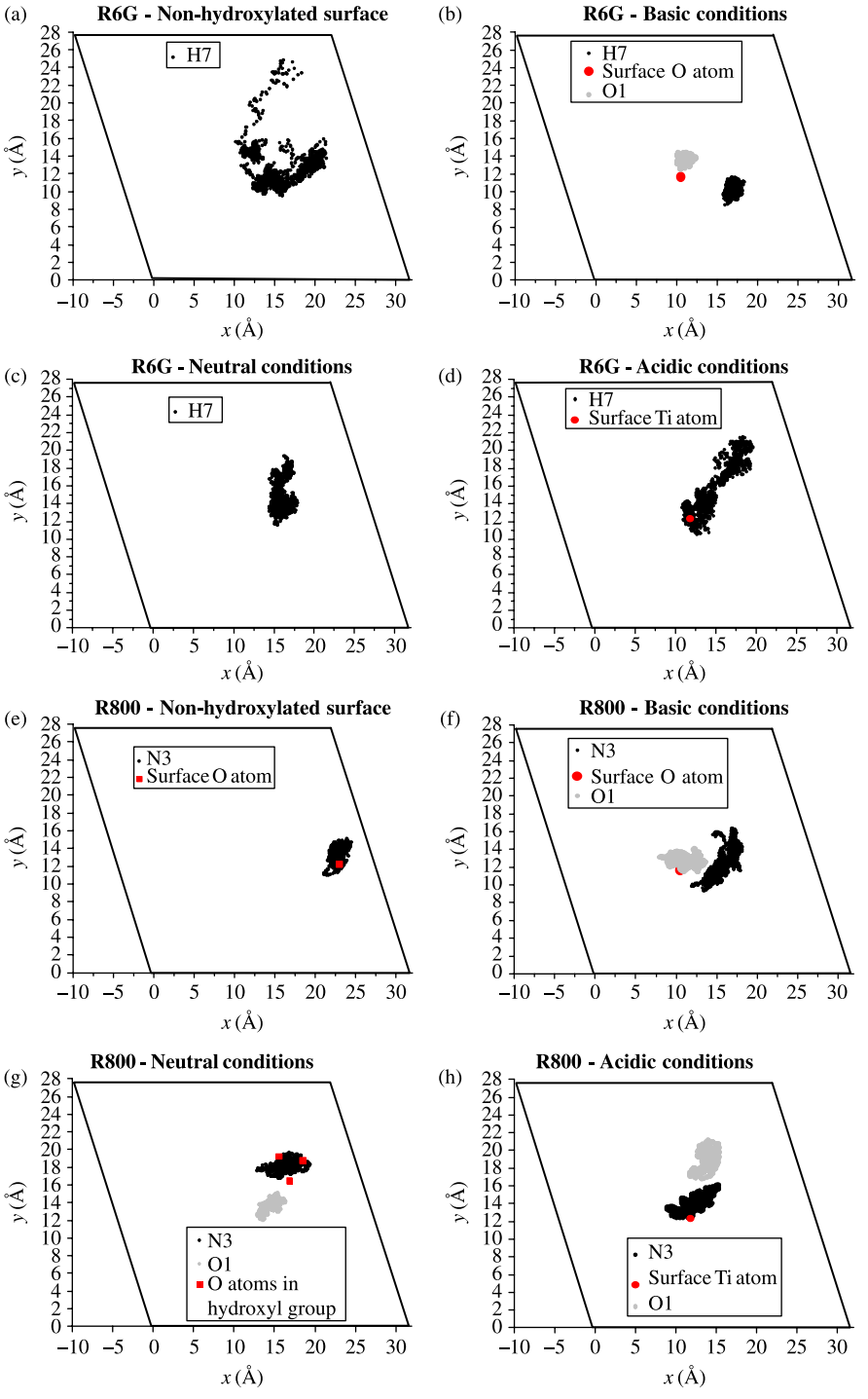

Figure 6. Plot of the values of the (x, y) coordinates of some relevant atoms, taken every 0.1 ps during the whole simulations. (a) R6G on non-hydroxylated surface. (b) R6G under basic conditions. (c) R6G under neutral conditions. (d) R6G under acidic conditions. (e) R800 on non-hydroxylated surface. (f) R800 under basic conditions. (g) R800 under neutral conditions. (h) R800 under acidic conditions.

at the surface interacts preferentially with the opposite side of the molecule, where most of the positive charge of the molecule is concentrated. It can be observed in Figure 6(f) that the N atom does not get close to the surface O atom. To represent the movement of the xanthene moiety, we have chosen the atom O1. It has a small negative charge ($-0.183e$), and is surrounded by positive charges, so the position of the O1 atom is oscillating around the surface O atom. Regarding the angles accounting for this interaction, the average values of both angles α and β are within the range

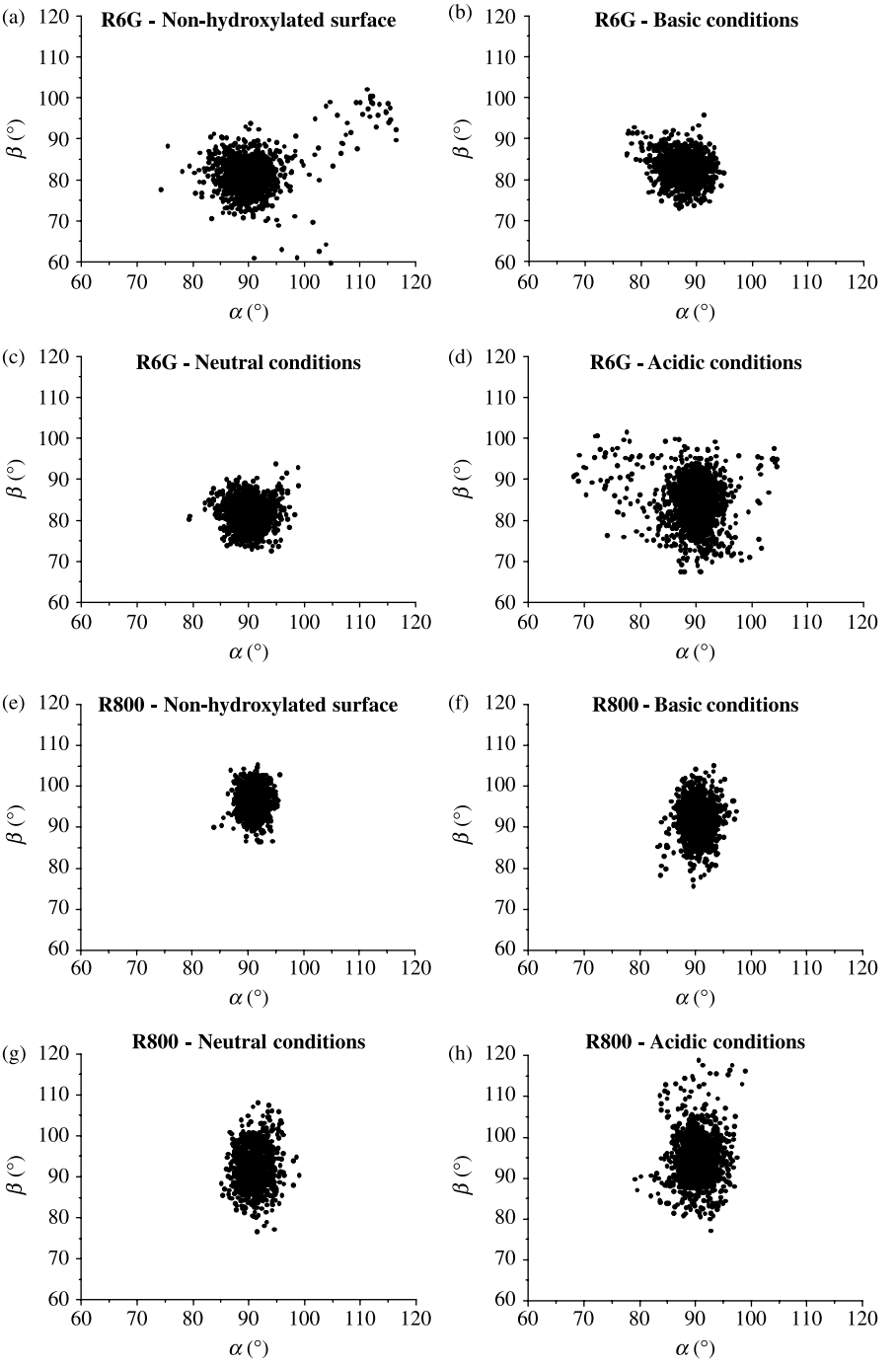

Figure 7. Values of the angles α and β during the simulations for the different simulations. α (β) is defined as the angle between the axis a (b) of the molecules (which is shown in Figure 2) and the z axis of the unit cell. (a) R6G on non-hydroxylated surface. (b) R6G under basic conditions. (c) R6G under neutral conditions. (d) R6G under acidic conditions. (e) R800 on non-hydroxylated surface. (f) R800 under basic conditions. (g) R800 under neutral conditions. (h) R800 under acidic conditions.

90°–92° (see Figure 8), which means that the molecule is basically lying parallel to the surface.

In the surface that models neutral conditions, the negatively charged site defect is not present, and the interaction between the rhodamine molecule and the surface is mainly due to their mutual van der Waals interactions. As a result, E_{ad} decreases from -51.6 to -33.2 kcal mol^{-1}. The negatively charged N atom in the nitrile group is now mainly attracted to the positively charged H atoms of the hydroxyl groups, and falls in the potential well created by the H atoms belonging to three adjacent hydroxyl groups. This can be seen in Figure 6(g)

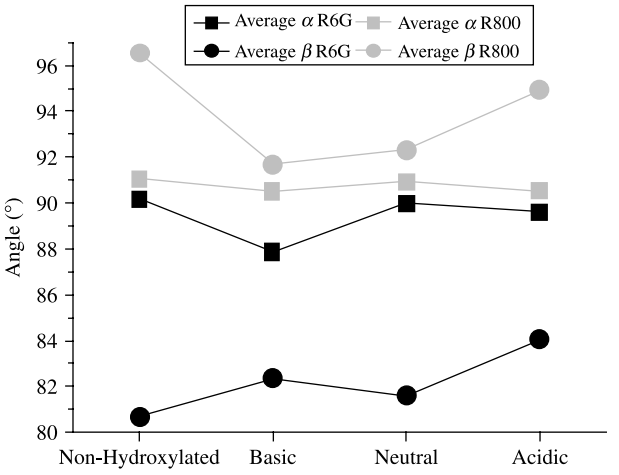

Figure 8. Average values of the angles α and β during the simulations.

where we have plotted the coordinates of the atoms N3 and O1 of the R800 molecules, as well as the coordinates of the O atoms of the hydroxyl groups, which are less mobile than the H atoms with which they are bonded. The distance from the superficial H atoms to the centre of the xanthene moiety, 2.82 Å, is roughly the same as in the case of adsorption under basic conditions, and the adsorption geometry in both cases is very similar. This similarity is also found for the values of the angles α and β, which lie within a range of 90°–92° (Figures 7(g) and 8), thus indicating that the adsorption is parallel to the surface.

Experimentally, the relatively high adsorption of R800 under acidic conditions (which is very similar to the level of adsorption in neutral conditions) is somewhat unexpected, because under these conditions, both the surface and the R800 molecule are positively charged. Our simulations provide a basis to understand why a significant adsorption takes place. The value of E_{ad} predicted

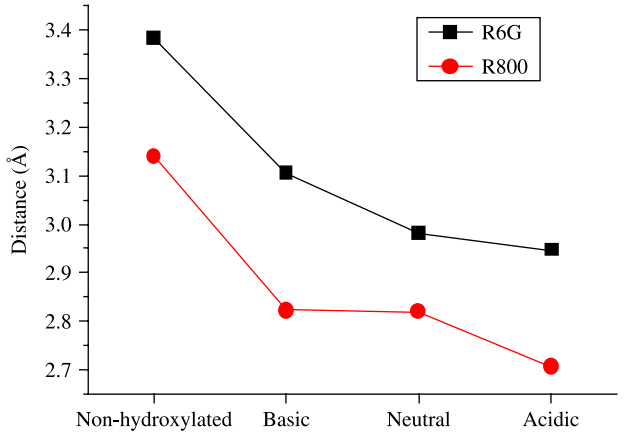

Figure 9. Average distance between the surfaces and the rhodamine molecules.

by our simulations is $-29.4\,\mathrm{kcal\,mol^{-1}}$, which is very close to the value obtained under neutral conditions, $-33.2\,\mathrm{kcal\,mol^{-1}}$. The reason why electrostatic repulsion between the two charged systems does not produce a significant decrease in the value of E_{ad} is due to the fact that the positive charge around the Ti atom at the surface does not interact directly with the positive charge of the rhodamine molecule. Instead, it is the negatively charged N atom of the nitrile group the one that is closer to it. Figure 6(h) shows that the positively charged region of the molecule (which surrounds the O1 atom) stays as far away as possible from the Ti atom, whereas the N3 atom is attracted by the positive charge of the Ti atom. There is a change in the angles of adsorption with respect to the cases of basic and neutral conditions. The average value of the angle α, 90°, is similar to the previous cases, but the average value of the angle β has increased to 95° (Figures 7(h) and 8). This is due to the mentioned attraction between the N3 atom and the surface Ti atom, which tends to keep them together. Indeed, this attraction induces a decrease in the distance between the molecule and the surface (which changes from 2.8 to 2.7 Å). Since the rest of the molecule cannot get closer to the hydroxyl groups of the surface, this effect results in an increase in the adsorption angle β, i.e. the position of the N3 atom is lower than that of the rest of the molecule. This particular geometrical arrangement has the net effect of creating an attraction between two positively charged systems.

4. Concluding remarks

The simulations reported here offer a preliminary atomistic insight into the adsorption processes on TiO_2 of two industrially relevant dye molecules, namely R6G and R800. The task of simulating TiO_2 surfaces is very challenging. Theoretical studies of the adsorption of molecules are often carried out by employing bare TiO_2 surfaces. Our results show that there are large differences in adsorption energies and geometries when the state of the surface is changed. Thus, for the two studied molecules, the adsorption energy on a hydroxylated surface is almost half of that calculated in the case of a bare surface. One of the greatest challenges regarding the simulation of TiO_2 surfaces is to model the effect of the different pHs. Using two models to simulate high and low pH conditions, we have calculated the adsorption energies of the two molecules under basic, neutral and acidic conditions. For R6G, the simulations predict a high energy of adsorption and therefore much adsorption under basic conditions, less adsorption under neutral conditions and practically no adsorption under acidic conditions. For R800, there is a high energy of adsorption under basic conditions, while the adsorption energies under neutral and acidic conditions are lower than the latter, but very similar to each other. These results are in qualitative agreement with the

experimental observations, which provides additional confidence on the ability of the simulations to model realistic adsorption conditions. However, despite this success in achieving a qualitative agreement between experimental and theoretical results, there are still many factors involved in the adsorption of molecules on TiO_2 which we have not taken into account. For example, we have studied the final states, in which the rhodamine molecules are adsorbed onto the dry surface, but we have not modelled the transition from the wet to the dry TiO_2 surface. This is an interesting process, since there is a loss of water molecules, while the rhodamine molecules are kept attached to the surface. Another relevant factor that influences the adsorption of rhodamine molecules is the presence of counterions [43,45]. On the other hand, there is a rich variety of ways in which rhodamine molecules can interact both in solution and on the surface, such as forming monomers, H-dimers, J-dimers, etc. [6–11], which have a great influence on the photoluminescence properties [21,46,47]. Thus, another interesting problem is to assess how the dimerisation process affects the adsorption on the surfaces. The ultimate goal of the inclusion of all these other effects would be to obtain a more accurate description of these systems, which could provide theoretical data to guide the experimental research. For these reasons, an intense theoretical work is being carried out in our group along this line.

Acknowledgements

We dedicate this work to the memory of José Antonio Mejías, an excellent friend and a good scientist, who put the first stones of this research line in our group. We will always remember him kindly. We thank the Ministry of Science and Education of Spain (project MAT 2007-65764/NAN2004-09317 and the CONSOLIDER INGENIO 2010-CSD2008-00023) and the Junta de Andalucía (projects TEP2275 and P07-FQM-03298) for the financial support. We would also like to thank the EU for the financial support provided by the EU contract no. 033793.

References

[1] R. Sasai, N. Iyi, T. Fujita, F.L. Arbeloa, V.M. Martinez, K. Takagi, and H. Itoh, *Luminescence properties of rhodamine 6G intercalated in surfactant/clay hybrid thin solid films*, Langmuir 20 (2004), pp. 4715–4719.

[2] F. Marlow, M.D. McGehee, D. Zhao, B.F. Chmelka, and G.D. Stucky, *Doped mesoporous silica fibers: A new laser material*, Adv. Mater. 11 (1999), pp. 632–636.

[3] D. Tleugabulova, Z. Zhang, Y. Chen, M.A. Brook, and J.D. Brennan, *Fluorescence anisotropy in studies of solute interactions with covalently modified colloidal silica nanoparticles*, Langmuir 20 (2004), pp. 848–854.

[4] L. Bahadur and P. Srivastava, *Efficient photon-to-electron conversion with rhodamine 6G-sensitized nanocrystalline* n-*ZnO thin film electrodes in acetonitrile solution*, Sol. Energy Mater. Sol. Cells 79 (2003), pp. 235–248.

[5] T. Ohishi, *An ethoxy-silano rhodamine B derivative and its application to surface coatings on display devices*, J. Non-Cryst. Solids 332 (2003), pp. 80–86.

[6] V. Martínez Martínez, F. López Arbeloa, J. Bañuelos Prieto, T. Arbeloa Lopez, and I. López Arbeloa, *Characterization of supported solid thin films of laponite clay. Intercalation of rhodamine 6G laser dye*, Langmuir 20 (2004), pp. 5709–5717.

[7] A.H. Gemeay, *Adsorption characteristics and the kinetics of the cation exchange of rhodamine-6G with Na^+-montmorillonite*, J. Colloid Interface Sci. 251 (2002), pp. 235–241.

[8] J. Bujdák, N. Iyi, and R. Sasai, *Spectral properties. Formation of dye molecular aggregates, and reactions in rhodamine 6G/layered silicate dispersions*, J. Phys. Chem. B 108 (2004), pp. 4470–4477.

[9] J. Bujdák and N. Iyi, *Molecular orientation of rhodamine dyes on surfaces of layered silicates*, J. Phys. Chem. B 109 (2005), pp. 4608–4615.

[10] V. Martínez, S. Salleres, J. Bañuelos, and F.L. Arbeloa, *Application of fluorescence with polarized light to evaluate the orientation of dyes adsorbed in layered materials*, J. Fluoresc. 16 (2006), pp. 233–240.

[11] F. del Monte, J.D. Mackenzie, and D. Levy, *Rhodamine fluorescent dimers adsorbed on the porous surface of silica gels*, Langmuir 16 (2000), pp. 7377–7382.

[12] A. Barranco and P. Groening, *Fluorescent plasma nanocomposite thin films containing nonaggregated rhodamine 6G laser dye molecules*, Langmuir 22 (2006), pp. 6719–6722.

[13] R. Vogel, P. Meredith, I. Kartini, M. Harvey, J.D. Riches, A. Bishop, N. Heckenberg, M. Trau, and H. Rubinsztein-Dunlop, *Mesostructured dye-doped titanium dioxide for micro-optoelectronic applications*, ChemPhysChem. 4 (2003), pp. 595–603.

[14] J.R. Sánchez-Valencia, A. Borrás, A. Barranco, V.J. Rico, J.P. Espinós, and A.R. González-Elipe, *Preillumination of TiO_2 and Ta_2O_5 photoactive thin films as a tool to tailor the synthesis of composite materials*, Langmuir 24 (2008), pp. 9460–9469.

[15] M. Kosmulski, *Chemical Properties of Material Surfaces*, Marcel Dekker, Inc., New York, 2001.

[16] B. O'Regan and M. Grätzel, *A low-cost, high-efficiency solar cell based on dye-sensitized colloidal TiO_2 films*, Nature 353 (1991), pp. 737–740.

[17] A. Hagfeldt and M. Grätzel, *Light-induced redox reactions in nanocrystalline systems*, Chem. Rev. 95 (1995), pp. 49–68.

[18] F. de Angelis, S. Fantacci, A. Selloni, M.K. Nazeeruddin, and M. Grätzel, *Time-dependent density functional theory investigations on the excited states of Ru(II)-dye-sensitized TiO_2 nanoparticles: The role of sensitizer protonation*, J. Am. Chem. Soc. 129 (2007), pp. 14156–14157.

[19] S.A. Tomás, S. Stolik, R. Palomino, R. Lozada, C. Persson, I. Pepe, and A. Ferreira da Silva, *Influence of rhodamine 6G doping on the optical properties of TiO_2 sol–gel films*, J. Appl. Phys. 98 (2005), 073516 (1–3).

[20] R. Sasai, T. Fujita, N. Iyi, H. Itoh, and K. Takagi, *Aggregated structures of rhodamine 6G intercalated in a fluor-taeniolite thin film*, Langmuir 18 (2002), pp. 6578–6583.

[21] J. Bujdák and N. Iyi, *Molecular aggregation of rhodamine dyes in dispersions of layered silicates: Influence of dye molecular structure and silicate properties*, J. Phys. Chem. B 110 (2006), pp. 2180–2186.

[22] K. Robbie and M.J. Brett, *Sculptured thin films and glancing angle deposition: Growth mechanics and applications*, J. Vac. Sci. Technol. A 15 (1997), pp. 1460–1465.

[23] M. Predota, A.V. Bandura, P.T. Cummings, J.D. Kubicki, D.J. Wesolowski, A.A. Chialvo, and M.L. Machesky, *Electric double layer at the rutile (1 1 0) surface. 1. Structure of surfaces and interfacial water from molecular dynamics by use of* ab initio *potentials*, J. Phys. Chem. B 108 (2004), pp. 12049–12060.

[24] A. Fortunelli and S. Monti, *Simulations of lipid adsorption on TiO_2 surfaces in solution*, Langmuir 24 (2008), pp. 10145–10154.

[25] S. Köppen, O. Bronkalla, and W. Langel, *Adsorption configurations and energies of amino acids on anatase and rutile surfaces*, J. Phys. Chem. C 112 (2008), pp. 13600–13606.

[26] A. Tilocca and A. Selloni, *Methanol adsorption and reactivity on clean and hydroxylated anatase (1 0 1) surfaces*, J. Phys. Chem. B 108 (2004), pp. 19314–19319.

[27] A. Tilocca, C. Di Valentin, and A. Selloni, *O_2 interaction and reactivity on a model hydroxylated rutile (1 1 0) surface*, J. Phys. Chem. B 109 (2005), pp. 20963–20967.

[28] A.V. Bandura and J.D. Kubicki, *Derivation of force field parameters for TiO_2–H_2O systems from* ab initio *calculations*, J. Phys. Chem. B 107 (2003), pp. 11072–11081.
[29] M. Matsui and M. Akaogi, *Molecular dynamics simulation of the structural and physical properties of the four polymorphs of TiO_2*, Mol. Simul. 6 (1991), pp. 239–244.
[30] G. Kresse and J. Joubert, *From ultrasoft pseudopotentials to the projector augmented-wave method*, Phys. Rev. B 59 (1999), pp. 1758–1775.
[31] J. Perdew, J. Chevary, S. Vosko, K. Jackson, M. Pederson, D. Singh, and C. Fiolhais, *Atoms, molecules, solids, and surfaces: Applications of the generalised gradient approximation for exchange and correlation*, Phys. Rev. B 46 (1992), pp. 6671–6687.
[32] G. Kresse and J. Hafner, Ab initio *molecular dynamics for liquid metals*, Phys. Rev. B 47 (1993), pp. 558–561.
[33] G. Kresse and J. Furthmuller, *Efficient iterative schemes for* ab initio *total-energy calculations using a plane-wave basis set*, Phys. Rev. B 54 (1996), pp. 11169–11186.
[34] G. Kresse and J. Furthmuller, *Efficiency of* ab-initio *total energy calculations for metals and semiconductors using a plane-wave basis set*, Comput. Mater. Sci. 6 (1996), pp. 15–50.
[35] H.J. Monkhorst and J.D. Pack, *Special points for Brillouin-zone integration*, Phys. Rev. B 13 (1976), pp. 5188–5192.
[36] S.L. Mayo, B.D. Olafson, and W.A. Goddard, *DREIDING: A generic force field for molecular simulations*, J. Phys. Chem. 94 (1990), pp. 8897–8909.
[37] D.E. Williams and S.R. Cox, *Nonbonded potentials for aza-hydrocarbons: The importance of the coulombic interaction*, Acta Cryst. B 40 (1984), pp. 414–417.
[38] D.E. Williams and D.J. Houpt, *Fluorine nonbonded potential parameters derived from crystalline perfluorocarbons*, Acta Cryst. B 42 (1986), pp. 286–295.
[39] U.C. Singh and P.A. Kollman, *An approach to computing electrostatic charges for molecules*, J. Comp. Chem. 5 (1984), pp. 129–145.
[40] B.H. Besler, K.M. Merz, Jr, and P.A. Kollman, *Atomic charges derived from semiempirical methods*, J. Comp. Chem. 11 (1990), pp. 431–439.
[41] M.J. Frisch, G.W. Trucks, H.B. Schlegel, G.E. Scuseria, M.A. Robb, J.R. Cheeseman, J.A.M. Jr, T. Vreven, K.N. Kudin, J.C. Burant, et al., *Gaussian 03*, Gaussian, Inc., Wallingford, CT, 2004.
[42] A.D. Becke, *Density-functional thermochemistry. III. The role of exact exchange*, J. Chem. Phys. 98 (1993), pp. 5648–5652.
[43] P. Capková, P. Malý, M. Pospísil, Z. Klika, H. Weissmannová, and Z. Weiss, *Effect of surface and interlayer structure on the fluorescence of rhodamine B–montmorillonite: Modeling and experiment*, J. Colloid Interface Sci. 277 (2004), pp. 128–137.
[44] J.D. Gale, *GULP: A computer program for the symmetry-adapted simulation of solids*, J. Chem. Soc. Faraday Trans. 93 (1997), pp. 629–637.
[45] Z. Klika, H. Weissmannová, P. Capková, and M. Pospísil, *The rhodamine B intercalation of montmorillonite*, J. Colloid Interface Sci. 275 (2004), pp. 243–250.
[46] F. López Arbeloa, R. Chaudhuri, T. Arbeloa López, and I. López Arbeloa, *Aggregation of rhodamine 3B adsorbed in Wyoming montmorillonite aqueous suspensions*, J. Colloid Interface Sci. 246 (2002), pp. 281–287.
[47] V. Martínez Martínez, F. López Arbeloa, J. Bañuelos Prieto, T. Arbeloa López, and I. López Arbeloa, *Characterization of rhodamine 6G aggregates intercalated in solid thin films of laponite clay. 1. Absorption spectroscopy*, J. Phys. Chem. B 108 (2004), pp. 20030–20037.